AGU PUBLICATIONS

JGR

Journal of Geophysical Research: Atmospheres

RESEARCH ARTICLE
10.1002/2016JD024886

Key Points:
- The first report of single-particle mass spectrometry measurements of fog droplet residues at ground level
- Most fog droplet residues are composed of elemental carbon
- Trimethylamine and hydroxymethanesulfonate are not found in the fog droplet residues

Supporting Information:
- Supporting Information S1

Correspondence to:
G. Zhang,
zhanggh@gig.ac.cn

Citation:
Bi, X., et al. (2016), In situ detection of the chemistry of individual fog droplet residues in the Pearl River Delta region, China, *J. Geophys. Res. Atmos.*, *121*, 9105–9116, doi:10.1002/2016JD024886.

Received 3 FEB 2016
Accepted 18 JUL 2016
Accepted article online 20 JUL 2016
Published online 3 AUG 2016

In situ detection of the chemistry of individual fog droplet residues in the Pearl River Delta region, China

Xinhui Bi[1], Qinhao Lin[1,2], Long Peng[1,2], Guohua Zhang[1], Xinming Wang[1], Fred J. Brechtel[3], Duohong Chen[4], Mei Li[5], Ping'an Peng[1], Guoying Sheng[1], and Zhen Zhou[5]

[1]State Key Laboratory of Organic Geochemistry and Guangdong Key Laboratory of Environmental Resources Utilization and Protection, Guangzhou Institute of Geochemistry, Chinese Academy of Sciences, Guangzhou, China, [2]University of Chinese Academy of Sciences, Beijing, China, [3]Brechtel Manufacturing Inc., Hayward, California, USA, [4]State Environmental Protection Key Laboratory of Regional Air Quality Monitoring, Guangdong Environmental Monitoring Center, Guangzhou, China, [5]Atmospheric Environment Institute of Safety and Pollution Control, Jinan University, Guangzhou, China

Abstract We use a single-particle aerosol mass spectrometer coupled with a ground-based counterflow virtual impactor to measure the chemical compositions of individual submicron fog droplet residues. This is the first report on single particle mass spectrometry measurements of fog droplet residual particles at ground level in an urban area. We show that most of the fog droplet residues were composed of elemental carbon (EC) (67.7%), followed by K-rich (19.2%) and mineral dust/metal (12.3%) particles. The predominance of EC-containing particles demonstrated that these particles could be effective fog nuclei and highlights the important influence of anthropogenic emissions on regional climate system. Compared with interstitial and ambient aerosols, nitrate was enhanced, sulfate was depressed, and ammonium- and organics-containing particles were hardly found in the fog droplet residues during fog events, suggesting that dust and metal particles containing nitrate may be preferentially activated and that ammonium and organics may not play important roles in fog formation in Guangzhou. We also present direct observational evidence that trimethylamine and hydroxymethanesulfonate are not found within fog droplet residues, although we previously observed enhanced gas-to-particle partitioning of these compounds by fog processing. Additionally, higher fraction or intensities of $[K]^+$, $[Fe]^+$, and $[SiO_3]^-$ were found in fog droplet residues than in ambient and interstitial particles.

1. Introduction

Fog can impair atmospheric visibility. The interactions between atmospheric pollutants and fog droplets may have substantial influence on peoples' daily lives, agriculture, and human health [*Butler and Trumble*, 2008; *Michna et al*., 2015; *Yamaguchi et al*., 2015]. Therefore, the physical and chemical processes of fog formation need to be elucidated. Fog water has been studied for decades, and most previous studies focused on offline measurements following the collection of bulk fog water. These studies showed that ammonium, sulfate, and nitrate are the primary inorganic species and that a considerable fraction of soluble organics exists in fog water [*Guo et al*., 2012; *Herckes et al*., 2015; *Kiss et al*., 2001; *Straub et al*., 2012]. The suspended insoluble particles that have been measured in fog water are dominated by water-insoluble organic matter and elemental carbon (EC) [*Giulianelli et al*., 2014; *Herckes et al*., 2013]. The limitations of bulk fog water measurements are that the samples are composed of a mixture of droplets, interstitial particles, and potential artifacts from shattered droplets. In contrast, the direct observation of activated fog droplets is rare. *Facchini et al*. [1999] reported that water-soluble species constitute a significant part of total carbon within fog droplets, whereas water-insoluble carbon species are preferentially found in the fog interstitial particles. *Hammer et al*. [2014] observed that the concentration of activated fog droplets was relatively low and that the nonactivated hydrated particles contributed significantly to the observed light scattering and, thus, the reduction in visibility. However, to date, the connection between the input particles and activated fog droplet properties has not been directly demonstrated. To accurately estimate the influence of anthropogenic activities on fog formation, it is critical to understand the factors that determine the ability of a particle to act as a fog droplet nucleus.

Freshly emitted carbonaceous particles from local sources are often relatively less hydrophilic, and the long-lived species associated with the atmospheric aging process may play a substantial role in the formation of fog/cloud droplets [*Straub et al*., 2012]. Indeed, the aging processes that the particles experience during

transport make them more hydrophilic and increase their fog-scavenging tendencies. Black carbon (BC) with relatively thick coatings was found to be efficiently incorporated into cloud droplets at the marine boundary layer [*Schroder et al*., 2015]. Organic species have also been shown to be incorporated in cloud droplets [*Sorooshian et al*., 2006, 2007]. The enhancement of sulfate and nitrate through various mechanisms has been observed to be important in the cloud formation process [*Hayden et al*., 2008; *Wonaschuetz et al*., 2012]. In addition, metals have been shown to influence the production of sulfate and organic species in fog/cloud droplets [*Coggon et al*., 2012; *Harris et al*., 2013; *Z. Wang et al*., 2014]. However, the formation mechanisms that affect the chemical compositions of fog at the ground level and fog/cloud processing at high altitudes may differ because the atmospheric conditions (e.g., meteorological conditions and pollution levels) are significantly different [*Michna et al*., 2015]. Additionally, *Dall'Osto et al*. [2009] suggested different formation mechanisms of aerosol species between fog interstitial particles and droplet residual particles that depend on parameters (e.g., oxidizing ability and source of aerosols) other than the water content, although these mechanisms are not fully understood. To date, fog formation remains poorly constrained with respect to input particle properties.

The physical characteristics of fog in the mountainous area of the Pearl River Delta (PRD) region have been observed and simulated [*Deng et al*., 2007]. However, few studies have addressed the chemical characteristics of fogs in urban areas in the PRD region. In this study, online measurements were performed using a single particle aerosol mass spectrometer (SPAMS) coupled with a ground-based counterflow virtual impactor (GCVI) to characterize the size-resolved chemical compositions of individual fog droplet residual particles in an urban area in the PRD region. Single particle mass spectrometry of fog interstitial particles has been performed previously at the same site [*Zhang et al*., 2012]. The present paper provides the in situ single-particle, dual-polarity mass spectrometry measurements of fog droplet residual particles at ground level. The differences in the chemical compositions of fog droplet residues and ambient aerosols after the fog period are also discussed. To the best of our knowledge, this is the first report of the application of a single-particle mass spectrometer to study the activated particles responsible for fog droplet formation at ground level in an urban area.

2. Experiments

2.1. GCVI

A GCVI inlet system (GCVI Model 1205, Brechtel Mfg. Inc.) was used to sample the fog droplets. CVI has been extensively used to collect fog/cloud droplet residues in fog or cloud field measurement campaigns [*Hayden et al*., 2008; *Roth et al*., 2016; *Sorooshian et al*., 2013; *Zelenyuk et al*., 2010]. The characterization of CVI performed using a BMI Model 1204 is described by *Shingler et al*. [2012]. Similarly, a small wind tunnel was used to accelerate droplets and unactivated aerosols to velocities between 50 and 120 m s^{-1} (100 m s^{-1} was set in this study) immediately upstream of the CVI sampling tip. Only droplets exceeding a certain controllable size (or cut size) can pass through the counterflow, exit the CVI tip, and enter the evaporation chamber (with an air flow temperature at 40°C). In this chamber, the associated water is removed, leaving the dry residual particles that act as fog nuclei. Previous field measurements observed that median size of cloud/fog droplets is approximately 10 μm [*Quan et al*., 2011; *Shingler et al*., 2012]. In this study, the cut size was set to 8 μm, and the particle transmission efficiency was 50% [*Shingler et al*., 2012]. The observation of fog/cloud droplet residue is affected by the possibility of volatilization of some compounds due to the heating required to dry the droplets in the CVI [*Hayden et al*., 2008; *Prabhakar et al*., 2014; *Youn et al*., 2015].

2.2. Aerosol Sampling

Sampling was performed at the Guangzhou Institute of Geochemistry (GIG), Chinese Academy of Sciences (CAS). It is an urban site, surrounded by a highway and an expressway, and is situated 2 km away from the central business district. The dominant primary sources near the site are traffic and industry, with additional impact from harvest biomass burning [*Chan and Yao*, 2008; *Tao et al*., 2012]. In the last few decades, substantial atmospheric pollution events have been reported in this area because of the rapid urbanization and industrialization of the city [*Chan and Yao*, 2008; *Tao et al*., 2012].

This study is a part of a CAS research project called "Formation Mechanism and Control Strategies of Haze in China," which aims to clarify the key physical and chemical mechanisms of regional fog/haze formation and

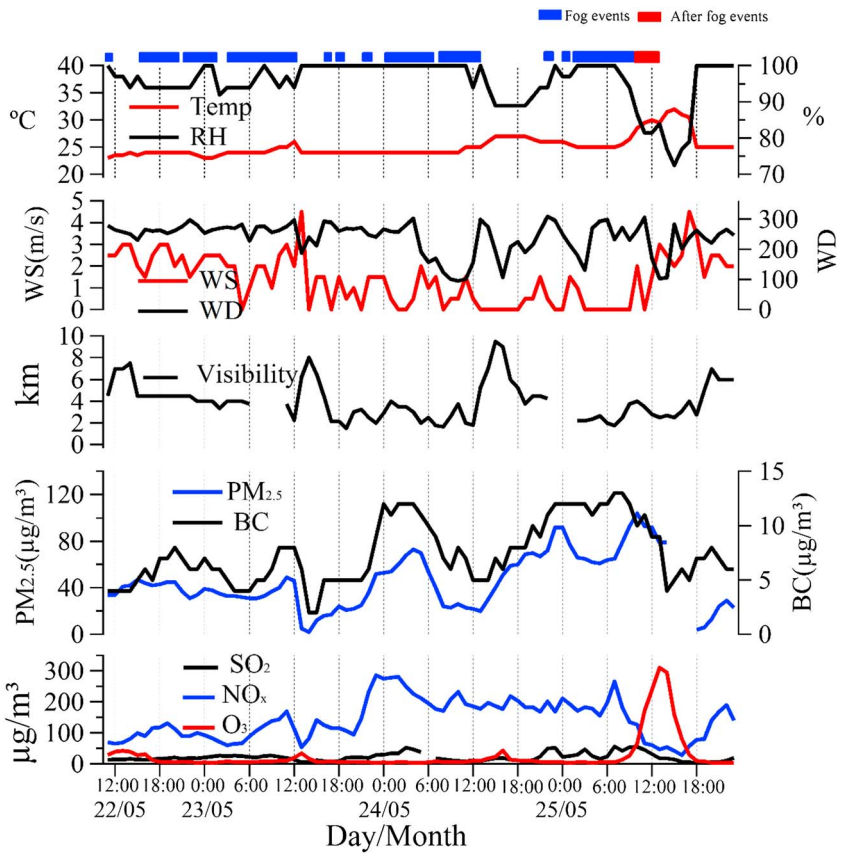

Figure 1. Temporal profiles (1 h resolution) of the mass concentrations of $PM_{2.5}$, BC, and gaseous pollutants (SO_2, NO_x, and O_3) and important meteorological parameters, including Temp, RH, WD, and WS, during 22–25 May 2015.

identify key pollutants and emission sources. During the campaign, fog droplet residual particles were sampled on top of a nine-story building. GCVI-SPAMS was deployed at GIG for 4 days (22 May to 25 May 2015). An upper limit visibility threshold of 5 km and a lower limit relative humidity (RH) threshold of 95% were set in the GCVI software to reliably identify the presence of fog. It is also noted that during most fog events, RH remained stable at 100%, as illustrated in Figure 1. Therefore, it is reasonable to assume that all dried particles in the droplets $> 8\,\mu m$ were activated as fog nuclei. Additionally, the GCVI system rainfall detector was used to exclude rainy periods. When fog occurred without precipitation, sampling was triggered automatically by the GCVI control software.

Fog droplet residual particles collected by the GCVI were subsequently analyzed by the downstream SPAMS (Hexin Analytical Instrument Co., Ltd. (Guangzhou, China)) for size-resolved chemical composition and by a condensation particle counter (CPC, Model 1500 Aerosol Generation and Monitoring System, MSP cooperation, MN, USA) for concentration. Online measurement of black carbon (BC) is conducted by a Multiangle Absorption Photometer (MAAP) (Model 5012, Thermo Fisher Scientific Inc.), based on the optical absorption and scattering of light by aerosols sampled on a filter tape [*Petzold et al.*, 2005]. Other air quality parameters (i.e., $PM_{2.5}$, NO_x, SO_2, and O_3) were also measured. Details for the instrumentation can be found in the supporting information.

Over the course of the campaign, the SPAMS collected an intermittent data set because the ambient particles between fog events were not sampled. Figure 2 shows the overall size statistics of the fog droplet residues, ambient particles after fog events, and interstitial particles detected during the previous study [*Zhang et al.*, 2012]. Because the particle-detection efficiency of the SPAMS is strongly dependent on the particle size [*Zhang et al.*, 2013], the number count does not represent the actual atmospheric concentration. In total, positive and negative ion mass spectra were collected for 1305 fog droplet residues with vacuum aerodynamic diameters (d_{va}) between 200 and 1100 nm. Because the low number of analyzed fog droplet residues limits the measurement statistics, we do not extend our analysis to the

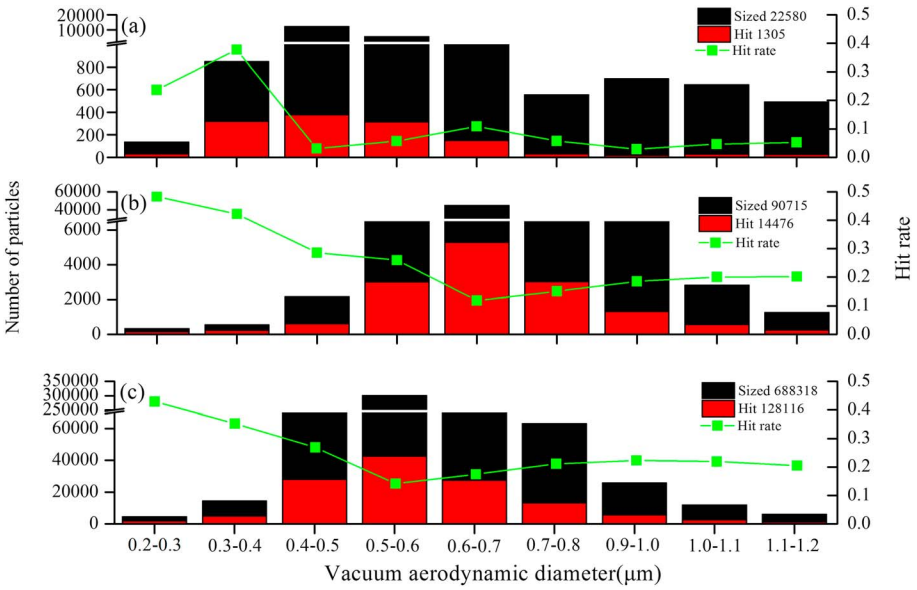

Figure 2. Histograms of the SPAMS-sized particles (black) and hit particles with polarity spectra shown in red and the hit rate indicated by the dotted green line: (a) fog residues, (b) ambient particles after fog events, and (c) interstitial particles (detected in 2010) [*Zhang et al*., 2012].

differences between single fog events. Instead, an average analysis covering all the fog events is presented. The average concentrations of the fog residual droplets and ambient particles were 0.37 cm^{-3} and 2860 cm^{-3}, respectively. Their average ratio was approximately 0.0001, indicating that instances of particle breakthrough and small particle contamination were absent [*Shingler et al*., 2012]. According to the calculation suggested by *Shingler et al*. [2012], the enhancement factor of particles measured by CVI was estimated to be approximately 5.25. It should also be noted that the concentrations measured by the CPC between the fog events might be underestimated because particles were sampled through the long pipe (~10 m) of the GCVI without pumping when the GCVI was off. Given these two factors, the ratio should be even lower, further indicating the negligible influence of particle contamination. After the fog period, 14,476 ambient particles were analyzed by the SPAMS over a period of 3 h for comparison. Statistically insufficient numbers of the fog residuals (1305) relative to the ambient particles (14,476) may restrictedly reflected the difference between the fog residuals and the ambient particles.

2.3. Data Analysis

An adaptive resonance theory-based neural network algorithm (ART-2a) was applied to cluster individual particles based on the presence and intensity of ion peaks in the single-particle mass spectrum, with a vigilance factor of 0.7, a learning rate of 0.05, and 20 iterations [*Zhang et al*., 2013]. The ART-2a algorithm generated 27 clusters used to describe the data set. By manually merging similar clusters, five major particle types with distinct chemical patterns were obtained, representing ~99.2% of the population of detected particles. The remaining particles were grouped together as "Other" in this study.

3. Results and Discussion

3.1. General Characteristics

Precipitation fog is formed by rain that falls from warmer air masses down to colder air masses and evaporates and is considered to be the main fog type in this study. The evaporative cooling and additional water vapor in the atmosphere are the main contributors to fog events [*Hammer et al*., 2014]. Figure 1 shows the temporal variations (1 h resolution) of meteorological parameters, including temperature (Temp), RH, wind direction (WD), wind speed (WS), visibility, and air quality parameters (i.e., $PM_{2.5}$, NO_x, SO_2, O_3, and BC). During the field study, Temp, RH, and WS varied in the ranges of 23–32°C, 72–100%, and 0–4.5 m s^{-1}, with average values of 25°C, 96%, and 1.4 m s^{-1}, respectively. In general, Temp and O_3 concentrations peaked

Table 1. Summary of the SPAMS Classifications During the Fog Events (22 May–25 May 2015)

SPAMS Class	Number of Particles	Percentage of the Total Residues
EC-NaK	335	25.7
EC	284	21.8
EC-Metal	264	20.2
K-rich	251	19.2
Mineral dust/metal	161	12.3
Other	10	0.8

during 13:00–15:00 and reached minimum values at night, whereas the variation of RH showed the opposite trend. The concentration peaks for $PM_{2.5}$ and BC were typically observed at nighttime and were associated with meteorological conditions facilitating the accumulation of pollutants. It should be noted that BC was optically measured by the MAAP and not by the SPAMS, which was used to measure EC in the fog residual particles. The air was stagnant during sampling, as confirmed by the low WS, and thus, the influence of local sources is reflected. The average SO_2 concentration during the fog events was 22 $\mu g\ m^{-3}$. The NO_x concentration peaked (281 $\mu g\ m^{-3}$) on 24 May. Back trajectories calculated with the Hybrid Single-Particle Lagrangian Integrated Trajectory (HYSPLIT) transport model (http://ready.arl.noaa.gov/HYSPLIT.php) showed that a relatively stagnant air mass was present at the site on 24 May (Figure S1), consistent with high levels of NO_x and $PM_{2.5}$ characteristic of local emissions. The pollution levels during and after fog were similar and were primarily controlled by local emissions with high levels of BC and $PM_{2.5}$. However, an elevated level of O_3 and decrease in level of NO_x were observed after the fog period, which is mainly due to the beginning of sunny scenario and the associated fog dissipation.

The SPAMS allowed for the detection of individual fog droplet residual particles in real time. The average digitized mass spectra of fog droplet residual particles are illustrated in Figure S2. The dominant peaks corresponded to potassium (K^+), sodium (Na^+), and carbon cluster ions (e.g., m/z $\pm 12[C]^{+/-}$, $\pm 36[C_3]^{+/-}$, $\pm 48[C_4]^{+/-}$, $\pm 60[C_5]^{+/-}$, …) in the positive mass spectra, whereas sulfate, nitrate, OH^-, CN^-, and the carbon cluster ions generated the most common negative-ion peaks. The other species included metallic elements, such as iron (Fe^+). The complex mixture of these particles could be attributed to different sources and/or the extensive processing of fog droplet residue particles. As much as 95% of the fog droplet residual particles were found to consist of internal mixtures of secondary inorganic species (sulfate and/or nitrate) in variable amounts, indicating secondary processing [*Moffet and Prather*, 2009].

3.2. Chemical Characterization of Fog Droplet Residues

The chemical patterns of the analyzed fog residual particles were illustrated by classifying the particles into six distinct groups. The detected number and number fractions of various particle types are listed in Table 1, and their average mass spectra are shown in Figure 3. EC-containing particles, identified by the intense ion signals from EC cluster ions, accounted for the largest fraction (67.7%) of the fog droplet residues. Three EC-containing particle types were observed: (1) the internally mixed EC and sodium/potassium salt (EC-NaK) type, (2) the EC type, and (3) the internally mixed EC and metal species (EC-Metal) type. The EC-NaK type was associated with dominant carbon cluster ions, nitrate, and sulfate in the negative spectra and the dominant $23[Na]^+$ and $39[K]^+$ peaks in the positive spectra. These particles constituted the most abundant type, comprising 25.7% by number of the total particles, and are probably attributable to coal combustion (unpublished data). The EC-type particles were dominated by the distinct EC cluster ions, which likely arose from diesel exhaust [*Li et al.*, 2013], and mainly associated with sulfate. They accounted for 21.8% of all the clustered particles by number. The internally mixed EC and metal species (EC-Metal) type was mainly mixed with nitrate and accounted for 20.2% by number of the clustered particles. The associated metallic species were mainly $39[K]^+$, $23[Na]^+$, and $56[Fe]^+$, likely produced by the metal industry [*Taiwo et al.*, 2014]. The EC-containing particles were found to be internally mixed with sulfate and nitrate, indicating some degree of atmospheric aging or fog processing [*Dall'Osto et al.*, 2009; *Ram et al.*, 2012; *Yuan et al.*, 2015].

In addition to EC-containing particles, K-rich and mineral dust/metal particles were also identified. The K-rich type mainly contained $39[K]^+$ and nitrate ($-46[NO_2]^-$ and $-62[NO_3]^-$) and accounted for 19.2% of the total particles. These particles were attributed to traffic emissions and/or residential wood smoke [*Taiwo et al.*, 2014]. The mineral dust/metal type, with strong peaks at m/z $56[Fe]^+$, $55[Mn]^+$, $60[SiO_2]^-$, and $76[SiO_3]^-$, was mainly associated with nitrate and represented 12.3% of the total particles. The positive-ion mass spectral signature of the remaining particles (Other type) showed organic fragments

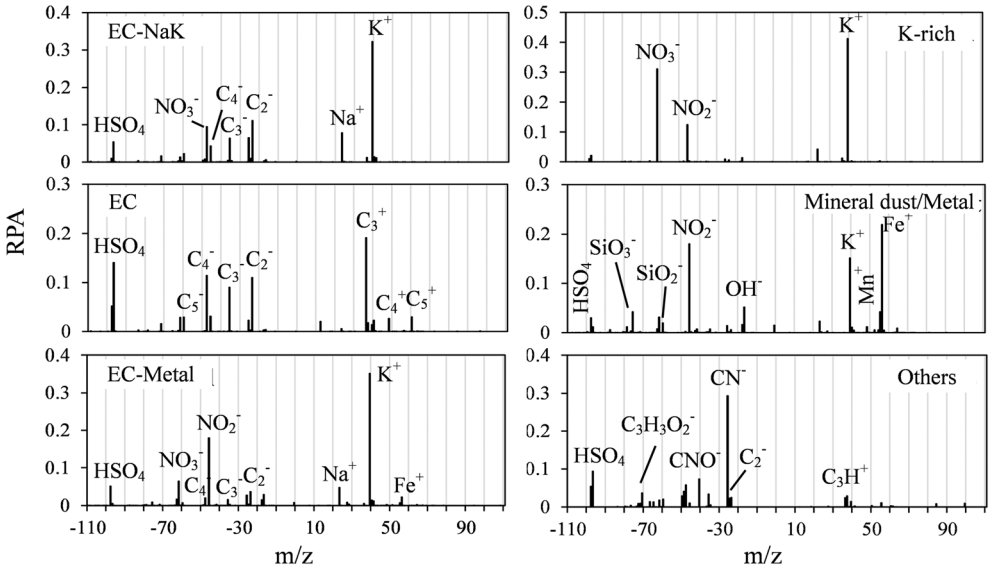

Figure 3. Average mass spectra of the major particle types identified in the fog droplet residues. The RPA is the relative peak area of each particle type.

at m/z 37[C_3H^+]. Additionally, very intense −26[$CN]^-$ and −42[$CNO]^-$ signatures were observed in the Other type, indicating the contribution of organic nitrogen [*Murphy et al.*, 2006]. However, this type only accounted for 0.8% of all the particles, suggesting that they contribute negligibly to fog formation.

The number fraction (Nf) for each particle type was found to be highly dependent on d_{va} (Figure 4). The EC and EC-NaK types showed similar distributions, with Nf decreasing as d_{va} increases. Although these types dominated the particles (with Nf > 82.5%) detected between 0.2 and 0.4 μm, the EC-Metal, K-rich, and mineral dust/metal types dominated (52–80%) in the size range of 0.5–0.8 μm. Notably, only droplet residues in the size range of 0.2–1.1 μm were detected in this study, but the results are still representative for all droplet residues. A study performed near Paris on the size-dependent particle activation of fog droplets revealed that the dry activation diameters were between 300 and 400 nm and that above this range, the activation fraction of particles exceeded 50% [*Hammer et al.*, 2014].

3.3. Comparison With Previous Fog/Cloud Measurements

Fog water has been observed to be dominated by sulfate, nitrate, and ammonium in many areas [*Guo et al.*, 2012; *Herckes et al.*, 2015, and references therein; *Michna et al.*, 2015]. *Herckes et al.* [2013] reviewed the measurements of organic matter in fog and cloud water, and some extremely high concentrations of organic matter have been observed in fog and cloud impacted by agriculture or biomass burning. In this study, the SPAMS analysis indicates that the fog droplet residues were dominated by EC, sulfate, and nitrate. The

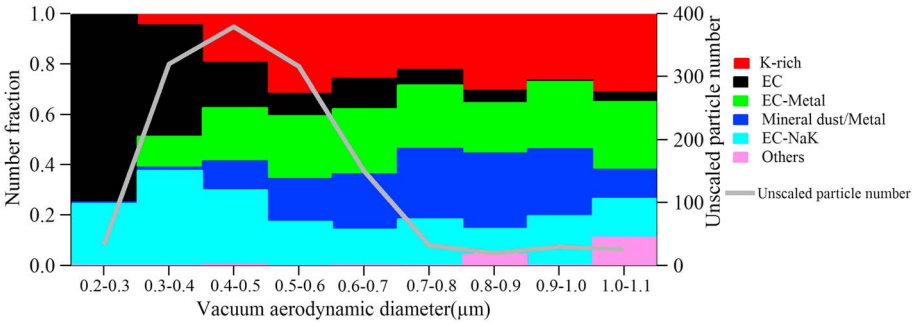

Figure 4. Size-resolved number fraction distributions of the particle types in fog droplet residues (100 nm resolution) throughout the sampling period.

overwhelming majority (~98%) of these residual particles appear to contain particles no apparent ammonium or organics. Ammonium was observed to be one of the most abundant ions in fog samples collected in Pennsylvania (USA), the Swiss Alps, and Japan [*Michna et al*., 2015; *Straub et al*., 2012; *Yamaguchi et al*., 2015]. The dominance of organic particles in the nonrefractory aerosol components of cloud droplet residues has also been reported [*Hao et al*., 2013; *Zelenyuk et al*., 2010]. However, the depletion of organics in cloud droplet residues was observed at a central European mountain site [*Roth et al*., 2016]. It should be noted that the absence of ammonium and organics is partly because of their volatile natures [*Prabhakar et al*., 2014; *Youn et al*., 2015]. However, this effect could not be significant because the temperature was set to 40°C to evaporate the associated water in fog droplets in this study. Previously, a volatility study demonstrated that ammonium nitrate/sulfate and most organics are unlikely to be evaporated when the particles are heated to temperatures lower than 75°C [*Bi et al*., 2015]. Although the photolysis of metal-organic complexes could lead to the reduction of some organic compounds [*Sorooshian et al*., 2013], this was likely negligible during the campaign that mainly associated with overcast or rainy days. Therefore, the absence of ammonium and organics in this study suggests that these species do not play significant roles in fog formation in Guangzhou.

Aqueous phase formation of secondary organic matter in fog process has been reported in the literatures [*Giulianelli et al*., 2014; *Kaul et al*., 2011; *Lim et al*., 2010]. Indeed, such formation has been observed via airborne measurements using a CVI and cloud water measurements [*Sorooshian et al*., 2006, 2007; *Z. Wang et al*., 2014]. *Rehbein et al*. [2011] demonstrated that cloud/fog processing could enhance the gas-to-particle partitioning of trimethylamine (TMA), which is highly dependent on aerosol water content. The concentration of particles containing hydroxymethanesulfonate (HMS), which can be used as a tracer for aqueous phase fog processing, has also been shown to sharply increase during fog events [*Dall'Osto et al*., 2009; *Zhang et al*., 2012]. We did observe enhanced TMA-containing particles in fog events during a 2010 sampling campaign using SPAMS without GCVI at the same sampling site [*Zhang et al*., 2012]. However, we observed the absence of TMA- and HMS-containing particles in the fog droplet residues. Therefore, our results imply that TMA and HMS might be produced on the surfaces of unactivated interstitial particles, suggesting that their formation mechanisms depend on parameters other than the water content [*Dall'Osto et al*., 2009]. However, this finding might also be partially attributable to the volatilization of these species during droplet evaporation [*Prabhakar et al*., 2014; *Youn et al*., 2015], which is beyond the scope of this work and needed to be better addressed in future studies.

3.4. Comparison With Ambient Particles Sampled After Fog Events

The mass spectra of the droplet residues, the ambient particles after fog events, and interstitial particles collected previously are compared in Figure 5. The formation of particulate sulfate and organics decreased and that of nitrate increased in fog droplets during fog events, rather than in interstitial particles and ambient particles, indicating that nitrate-containing particles are preferentially activated as fog droplets [*Prabhakar et al*., 2014]. It should be noted that although elevated O_3 level and decreased NO_x level (Figure 1) after the fog period might lead to potential formation of secondary species (i.e., sulfate, nitrate, and secondary organics), this conclusion could be still validated from the comparison between droplet residues and interstitial particles, as shown in Figure 5b. *Drewnick et al*. [2007] suggested that high contents of nitrate, rather than sulfate, in the initial particles results in more efficient activation into cloud droplets. A closer look at size distribution of nitrate-containing fog droplet residues showed that nitrate is mostly associated with larger particles comprised of dust and metals, including potassium (Figure S3). However, *Zelenyuk et al*. [2010] found that droplet residuals had higher sulfate contents than interstitial particles. Therefore, further examination of the activation of nitrate- and sulfate-containing aerosols is required to explain these different behaviors. The detected markers for organics ($37[C_3H]^+$) and ammonium ($18[NH_4]^+$) in fog droplet residues were significantly lower than those in ambient particles after fog events and in interstitial particles, further indicating that these species are less important for fog formation, as discussed in section 3.3, or that they predominantly existed in smaller cloud condensation nuclei (CCN) [*Rose et al*., 2011] not sampled by the SPAMS.

Although previous field observations noted lead enhancement in cloud residues [*Roth et al*., 2016], we did not find higher lead concentrations in the fog droplet residues in this study. Higher intensities of $[K]^+$ and $[Fe]^+$ were detected compared to unactivated particles (Figure 5), suggesting their importance in urban fog events. Additionally, a higher fraction of $[SiO_3]^-$, a tracer for mineral dust [*Kamphus et al*., 2010], was

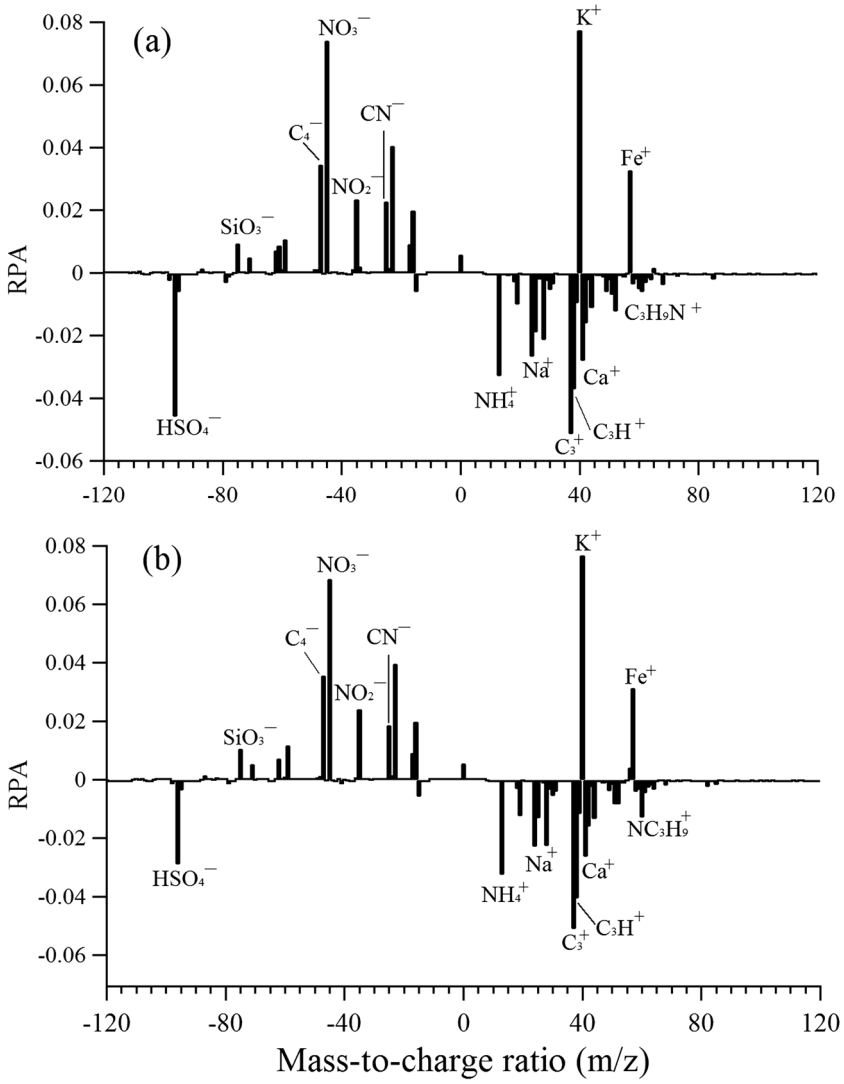

Figure 5. (a) Difference between the average mass spectra of the fog droplet residual and ambient particles after fog and (b) the fog droplet residual and interstitial particles.

identified in fog droplet residues than in ambient or interstitial particles, indicating its activity as fog nuclei. Previous measurements using single-particle mass spectrometers in the Swiss Alps showed that mineral dust had a low abundance in cloud droplet residues [*Kamphus et al.*, 2010]. Therefore, the presence of metals and mineral dust in fog residues most likely depends on the local sources of these materials. The comparison presented in Figure 5 should not be regarded as quantitative because we are comparing fog droplet residue compositions from one period with the ambient particle compositions from another. This is because the origins of the air masses and particle sources may be different.

3.5. Mixing States of Fog Droplet Residues With Secondary Species

More abundant fractions of sulfate signals were found for EC-NaK (76.4%) and EC (83.4%), as shown in Figure 6, and less abundant fractions of sulfate (35.1–59.0%) were present in the other particle types. For EC-Metal, SO_2 oxidation catalyzed by the natural in cloud oxidation of transition metal ions might be the dominant pathway of sulfate formation [*Harris et al.*, 2013]. For EC-NaK and EC, sulfate formation likely occurred before the particles were activated because in the absence of sulfate, the particles should be less hydrophilic. Therefore, we suspect that some amount of sulfate was formed via the oxidation of sulfur during combustion, which then condensed onto the existing EC particles in the plume [*Moffet and Prather*, 2009; *Zaveri et al.*, 2010]. Additionally, the rainy periods around the fog events were unfavorable for SO_2 oxidation

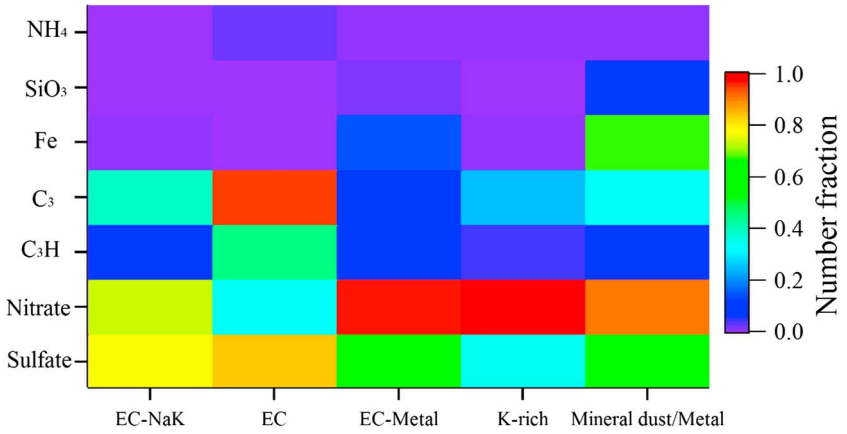

Figure 6. Nf values of several selected markers associated with the various particle types, indicated by different colors.

by OH radicals [*Xiao et al*., 2009]. It should also be noted that once activated, the oxidation of SO_2 by O_3 and/or H_2O_2 may further contribute to the observed sulfate [*Zelenyuk et al*., 2010].

Our observations also indicate that some fraction of sulfate should exist in the form of sulfuric acid rather than ammonium sulfate salts [*Zhang et al*., 2013] because very little ammonium was detected. Measurements taken in a power plant plume also showed that aerosol species were internally mixed and that the particles were acidic [*Zaveri et al*., 2010]. Compared to the EC-NaK and EC types, over 90% of EC-Metal, mineral dust/metal, and K-rich particles contained nitrate (Figure 6). The preferential enrichment of nitrate in alkaline particles indicates that nitrate tended to be formed through partitioning and heterogeneous/aqueous chemistry of nitric acid and other precursors [*Li and Shao*, 2009]. The sulfate in the fog droplet residues was also found to be in slightly smaller particles compared to nitrate (Figure S4). This trend is opposite to that reported in cloud measurements [*Hayden et al*., 2008] and might be explained by the different formation mechanisms of these species in fog and cloud measurements. *Hayden et al*. [2008] suggested that the formation of nitrate mainly occurred via gas-phase mass transfer, whereas sulfate forms through nucleation scavenging, leading to lower sizes of nitrate relative to sulfate. In this study, however, as discussed above, sulfate exists in the particles before becoming activated in the fog droplet, especially for the EC and EC-NaK types, whereas nitrate is preferentially associated with mineral dust/metal and K-rich particles with larger sizes (Figure S3).

3.6. Atmospheric Implications

In general, freshly emitted EC particles are less hydrophilic and do not substantially affect the fog droplet concentration [*Hammer et al*., 2014]. In this study, we observed the presence of EC in most fog residual particles. This result highlights the importance of EC in interactions with fog droplets, which represents one of the largest gaps in our understanding of the climate impact of EC [*Bond et al*., 2013]. However, few field studies have focused on this issue. *Roth et al*. [2016] reported a similar enhancement of EC in cloud droplet residues, rather than ambient particles; however, the Nf of EC-containing particles (~30%) in cloud droplet residues was lower than observed here. Based on indirect measurement, *Leng et al*. [2014] concluded that BC mass concentration had a strongly positive effect on the CCN concentration on foggy-hazy days. Using a single-particle soot photometer (SP2), *Schroder et al*. [2015] demonstrated that BC could be incorporated into cloud droplets. In contrast, *Facchini et al*. [1999] reported that water-insoluble carbon species preferentially exist in fog interstitial particles. *Zelenyuk et al*. [2010] observed negligible EC in cloud droplet residues by CVI-single-particle mass spectrometry. As described in the discussion above, the EC-containing particles were internally mixed with secondary inorganic compounds, primarily sulfate/nitrate. Furthermore, these EC-containing particles exhibited a high degree of mixing at our site [*Zhang et al*., 2013] and in polluted areas [*Huang et al*., 2011; *Q. Wang et al*., 2014; *Zhang et al*., 2014]. This mixing with soluble species enhanced their ability to act as CCN [*Khalizov et al*., 2009; *Roth et al*., 2016; *Zhang et al*., 2008] and should explain the enhancement of EC in the fog droplets. The contrasting observations of *Facchini et al*. [1999] and *Zelenyuk et al*. [2010] might be attributable to less EC processing and a lower degree mixing. Additionally, atmospheric conditions might also be responsible for the different observations between fog and cloud droplets at different altitudes. Further time-resolved measurements are required to correlate these results with meteorological measurements.

4. Conclusions

Here we present the first in situ chemically resolved measurements of fog droplet residual particles in China using GCVI-SPAMS. The results show that EC-containing particles were the dominant contributors to the fog droplet residues, implying their significant role in fog processing, at least at ground level in an urban area. Single-particle mixing state analysis revealed that alterations of the hygroscopic nature of the EC particles by internal mixing with secondary species are likely the main factor contributing to their activity as fog nuclei. The involvement of EC particles in fog formation highlights the importance of the interplay between anthropogenic emissions and the regional climate system. While dust and metal particles containing nitrate may be preferentially activated, ammonium and organics may not play important roles in fog formation in Guangzhou. TMA and HMS were not found within the fog droplet residues, although we previously observed enhanced the gas-to-particle partitioning of these species by fog processing.

Acknowledgments

This work was supported by the National Nature Science Foundation of China (91544101 and 41405131), the "Strategic Priority Research Program (B)" of the CAS (XDB05020205), and the Foundation for Leading Talents of the Guangdong Province Government. The authors gratefully acknowledge the NOAA Air Resources Laboratory (ARL) for the provision of the HYSPLIT transport and dispersion model and/or READY website (http://ready.arl.noaa.gov) used in this publication. The authors also greatly appreciate anonymous reviewers for their thoughtful suggestions that have helped substantially improve the manuscript. This is contribution from GIGCAS No.IS-2277. All the data can be obtained by contacting the corresponding author.

References

Bi, X. H., et al. (2015), Real-time and single-particle volatility of elemental carbon-containing particles in the urban area of Pearl River Delta region, China, *Atmos. Environ.*, *118*, 194–202, doi:10.1016/j.atmosenv.2015.08.012.

Bond, T. C., et al. (2013), Bounding the role of black carbon in the climate system: A scientific assessment, *J. Geophys. Res.-Atmos.*, *118*(11), 5380–5552, doi:10.1002/Jgrd.50171.

Butler, C. D., and J. T. Trumble (2008), Effects of pollutants on bottom-up and top-down processes in insect-plant interactions, *Environ. Pollut.*, *156*(1), 1–10, doi:10.1016/j.envpol.2007.12.026.

Chan, C. K., and X. Yao (2008), Air pollution in mega cities in China, *Atmos. Environ.*, *42*(1), 1–42, doi:10.1016/j.atmosenv.2007.09.003.

Coggon, M. M., et al. (2012), Ship impacts on the marine atmosphere: Insights into the contribution of shipping emissions to the properties of marine aerosol and clouds, *Atmos. Chem. Phys.*, *12*, 8439-8458, doi:10.5194/acp-12-8439-2012.

Dall'Osto, M., R. M. Harrison, H. Coe, and P. Williams (2009), Real-time secondary aerosol formation during a fog event in London, *Atmos. Chem. Phys.*, *9*(7), 2459–2469.

Deng, X., et al. (2007), Comprehensive analysis of the macro-and micro-physical characteristics of dense fog in the area south of the Nanling Mountains [in Chinese], *J. Trop. Meteorol.*, *23*(5), 424–434.

Drewnick, F., J. Schneider, S. S. Hings, N. Hock, K. Noone, A. Targino, S. Weimer, and S. Borrmann (2007), Measurement of ambient, interstitial, and residual aerosol particles on a mountaintop site in central Sweden using an aerosol mass spectrometer and a CVI, *J. Atmos. Chem.*, *56*(1), 1–20, doi:10.1007/s10874-006-9036-8.

Facchini, M. C., et al. (1999), Partitioning of the organic aerosol component between fog droplets and interstitial air, *J. Geophys. Res.*, *104*(D21), 26,821–26,832, doi:10.1029/1999JD900349.

Giulianelli, L., S. Gilardoni, L. Tarozzi, M. Rinaldi, S. Decesari, C. Carbone, M. C. Facchini, and S. Fuzzi (2014), Fog occurrence and chemical composition in the Po valley over the last twenty years, *Atmos. Environ.*, *98*, 394–401, doi:10.1016/j.atmosenv.2014.08.080.

Guo, J., et al. (2012), Characterization of cloud water chemistry at Mount Tai, China: Seasonal variation, anthropogenic impact, and cloud processing, *Atmos. Environ.*, *60*, 467–476, doi:10.1016/j.atmosenv.2012.07.016.

Hammer, E., et al. (2014), Size-dependent particle activation properties in fog during the ParisFog 2012/13 field campaign, *Atmos. Chem. Phys.*, *14*(19), 10,517–10,533, doi:10.5194/acp-14-10517-2014.

Hao, L., et al. (2013), Aerosol chemical composition in cloud events by high resolution time-of-flight aerosol mass spectrometry, *Environ. Sci. Technol.*, *47*(6), 2645–2653, doi:10.1021/es302889w.

Harris, E., et al. (2013), Enhanced role of transition metal ion catalysis during in-cloud oxidation of SO_2, *Science*, *340*(6133), 727–730, doi:10.1126/science.1230911.

Hayden, K. L., A. M. Macdonald, W. Gong, D. Toom-Sauntry, K. G. Anlauf, A. Leithead, S. M. Li, W. R. Leaitch, and K. Noone (2008), Cloud processing of nitrate, *J. Geophys. Res.*, *113*, D18201, doi:10.1029/2007JD009732.

Herckes, P., K. T. Valsaraj, and J. L. Collett (2013), A review of observations of organic matter in fogs and clouds: Origin, processing and fate, *Atmos. Res.*, *132*, 434–449, doi:10.1016/j.atmosres.2013.06.005.

Herckes, P., A. R. Marcotte, Y. Wang, and J. L. Collett (2015), Fog composition in the Central Valley of California over three decades, *Atmos. Res.*, *151*, 20–30, doi:10.1016/j.atmosres.2014.01.025.

Huang, X. F., et al. (2011), Black carbon measurements in the Pearl River Delta region of China, *J. Geophys. Res.*, *116*, D12208, doi:10.1029/2010JD014933.

Kamphus, M., M. Ettner-Mahl, T. Klimach, F. Drewnick, L. Keller, D. J. Cziczo, S. Mertes, S. Borrmann, and J. Curtius (2010), Chemical composition of ambient aerosol, ice residues and cloud droplet residues in mixed-phase clouds: Single particle analysis during the Cloud and Aerosol Characterization Experiment (CLACE 6), *Atmos. Chem. Phys.*, *10*(16), 8077–8095, doi:10.5194/acp-10-8077-2010.

Kaul, D. S., T. Gupta, S. N. Tripathi, V. Tare, and J. L. Collett (2011), Secondary organic aerosol: A comparison between foggy and nonfoggy days, *Environ. Sci. Technol.*, *45*(17), 7307–7313, doi:10.1021/es201081d.

Khalizov, A. F., R. Y. Zhang, D. Zhang, H. X. Xue, J. Pagels, and P. H. McMurry (2009), Formation of highly hygroscopic soot aerosols upon internal mixing with sulfuric acid vapor, *J. Geophys. Res.*, *114*, D05208, doi:10.1029/2008JD010595.

Kiss, G., B. Varga, A. Gelencser, Z. Krivacsy, A. Molnar, T. Alsberg, L. Persson, H. C. Hansson, and M. C. Facchini (2001), Characterisation of polar organic compounds in fog water, *Atmos. Environ.*, *35*(12), 2193–2200, doi:10.1016/S1352-2310(00)00473-8.

Leng, C., et al. (2014), Variations of cloud condensation nuclei (CCN) and aerosol activity during fog-haze episode: A case study from Shanghai, *Atmos. Chem. Phys.*, *14*(22), 12,499–12,512, doi:10.5194/acp-14-12499-2014.

Li, L., G. B. Tan, L. Zhang, Z. Fu, H. Q. Nian, Z. X. Huang, Z. Zhou, and M. Li (2013), Analysis of diesel exhaust particles using single particle aerosol mass spectrometry, *Chinese J. Anal. Chem.*, *41*(12), 1831–1836, doi:10.3724/Sp.J.1096.2013.30545.

Li, L., M. Li, Z. X. Huang, W. Gao, H. Q. Nian, Z. Fu, J. Gao, F. H. Chai, and Z. Zhou (2014), Ambient particle characterization by single particle aerosol mass spectrometry in an urban area of Beijing, *Atmos. Environ.*, *94*(0), 323–331, doi:10.1016/j.atmosenv.2014.03.048.

Li, W. J., and L. Y. Shao (2009), Observation of nitrate coatings on atmospheric mineral dust particles, *Atmos. Chem. Phys.*, *9*(6), 1863–1871.

Lim, Y. B., Y. Tan, M. J. Perri, S. P. Seitzinger, and B. J. Turpin (2010), Aqueous chemistry and its role in secondary organic aerosol (SOA) formation, *Atmos. Chem. Phys.*, *10*(21), 10,521–10,539, doi:10.5194/acp-10-10521-2010.

Michna, P., R. A. Werner, and W. Eugster (2015), Does fog chemistry in Switzerland change with altitude?, *Atmos. Res.*, *151*, 31–44, doi:10.1016/j.atmosres.2014.02.008.

Moffet, R. C., and K. A. Prather (2009), In-situ measurements of the mixing state and optical properties of soot with implications for radiative forcing estimates, *Proc. Natl. Acad. Sci. U.S.A.*, *106*(29), 11,872–11,877, doi:10.1073/pnas.0900040106.

Murphy, D. M., D. J. Cziczo, K. D. Froyd, P. K. Hudson, B. M. Matthew, A. M. Middlebrook, R. E. Peltier, A. Sullivan, D. S. Thomson, and R. J. Weber (2006), Single-particle mass spectrometry of tropospheric aerosol particles, *J. Geophys. Res.*, *111*, D23S32, doi:10.1029/2006JD007340.

Petzold, A., H. Schloesser, P. J. Sheridan, W. P. Arnott, J. A. Ogren, and A. Virkkula (2005), Evaluation of multiangle absorption photometry for measuring aerosol light absorption, *Aerosol Sci. Tech.*, *39*(1), 40–51.

Prabhakar, G., B. Ervens, Z. Wang, L. C. Maudlin, M. M. Coggon, H. H. Jonsson, J. H. Seinfeld, and A. Sorooshian (2014), Sources of nitrate in stratocumulus cloud water: Airborne measurements during the 2011 E-PEACE and 2013 NiCE studies, *Atmos. Environ.*, *97*, 166–173, doi:10.1016/j.atmosenv.2014.08.019.

Quan, J., Q. Zhang, H. He, J. Liu, M. Huang, and H. Jin (2011), Analysis of the formation of fog and haze in North China Plain (NCP), *Atmos. Chem. Phys.*, *11*(15), 8205–8214, doi:10.5194/acp-11-8205-2011.

Ram, K., M. M. Sarin, A. K. Sudheer, and R. Rengarajan (2012), Carbonaceous and secondary inorganic aerosols during wintertime fog and haze over urban sites in the Indo-Gangetic Plain, *Aerosol Air Qual. Res.*, *12*(3), 359–370, doi:10.4209/aaqr.2011.07.0105.

Rehbein, P. J. G., C. H. Jeong, M. L. McGuire, X. H. Yao, J. C. Corbin, and G. J. Evans (2011), Cloud and fog processing enhanced gas-to-particle partitioning of trimethylamine, *Environ. Sci. Technol.*, *45*(10), 4346–4352, doi:10.1021/es1042113.

Rose, D., et al. (2011), Cloud condensation nuclei in polluted air and biomass burning smoke near the mega-city Guangzhou, China—Part 2: Size-resolved aerosol chemical composition, diurnal cycles, and externally mixed weakly CCN-active soot particles, *Atmos. Chem. Phys.*, *11*, 2817–2836, doi:10.5194/acp-11-2817-2011.

Roth, A., J. Schneider, T. Klimach, S. Mertes, D. van Pinxteren, H. Herrmann, and S. Borrmann (2016), Aerosol properties, source identification, and cloud processing in orographic clouds measured by single particle mass spectrometry on a central European mountain site during HCCT-2010, *Atmos. Chem. Phys.*, *16*(2), 505–524, doi:10.5194/acp-16-505-2016.

Schroder, J. C., S. J. Hanna, R. L. Modini, A. L. Corrigan, S. M. Kreidenwies, A. M. Macdonald, K. J. Noone, L. M. Russell, W. R. Leaitch, and A. K. Bertram (2015), Size-resolved observations of refractory black carbon particles in cloud droplets at a marine boundary layer site, *Atmos. Chem. Phys.*, *15*(3), 1367–1383, doi:10.5194/acp-15-1367-2015.

Shingler, T., et al. (2012), Characterisation and airborne deployment of a new counterflow virtual impactor inlet, *Atmos. Meas. Tech.*, *5*(6), 1259–1269, doi:10.5194/amt-5-1259-2012.

Sorooshian, A., et al. (2006), Oxalic acid in clear and cloudy atmospheres: Analysis of data from International Consortium for Atmospheric Research on Transport and Transformation 2004, *J. Geophys. Res.*, *111*, D23s45, doi:10.1029/2005JD006880.

Sorooshian, A., N. L. Ng, A. W. H. Chan, G. Feingold, R. C. Flagan, and J. H. Seinfeld (2007), Particulate organic acids and overall water-soluble aerosol composition measurements from the 2006 Gulf of Mexico Atmospheric Composition and Climate Study (GoMACCS), *J. Geophys. Res.*, *112*, D13201, doi:10.1029/2007JD008537.

Sorooshian, A., Z. Wang, M. M. Coggon, H. H. Jonsson, and B. Ervens (2013), Observations of sharp oxalate reductions in stratocumulus clouds at variable altitudes: Organic acid and metal measurements during the 2011 E-PEACE campaign, *Environ. Sci. Technol.*, *47*(14), 7747–7756, doi:10.1021/es4012383.

Straub, D. J., J. W. Hutchings, and P. Herckes (2012), Measurements of fog composition at a rural site, *Atmos. Environ.*, *47*, 195–205, doi:10.1016/j.atmosenv.2011.11.014.

Taiwo, A. M., R. M. Harrison, D. C. S. Beddows, and Z. Shi (2014), Source apportionment of single particles sampled at the industrially polluted town of Port Talbot, United Kingdom by ATOFMS, *Atmos. Environ.*, *97*(0), 155–165, doi:10.1016/j.atmosenv.2014.08.009.

Tao, J., Z. X. Shen, C. S. Zhu, J. H. Yue, J. J. Cao, S. X. Liu, L. H. Zhu, and R. J. Zhang (2012), Seasonal variations and chemical characteristics of sub-micrometer particles (PM1) in Guangzhou, China, *Atmos. Res.*, *118*, 222–231, doi:10.1016/j.atmosres.2012.06.025.

Wang, Q., R. J. Huang, J. Cao, Y. Han, G. Wang, G. Li, Y. Wang, W. Dai, R. Zhang, and Y. Zhou (2014), Mixing state of black carbon aerosol in a heavily polluted urban area of China: Implications for light absorption enhancement, *Aerosol Sci. Tech.*, *48*, 689–697, doi:10.1080/02786826.2014.917758.

Wang, Z., A. Sorooshian, G. Prabhakar, M. M. Coggon, and H. H. Jonsson (2014), Impact of emissions from shipping, land, and the ocean on stratocumulus cloud water elemental composition during the 2011 E-PEACE field campaign, *Atmos. Environ.*, *89*, 570–580, doi:10.1016/j.atmosenv.2014.01.020.

Wonaschuetz, A., A. Sorooshian, B. Ervens, P. Y. Chuang, G. Feingold, S. M. Murphy, J. de Gouw, C. Warneke, and H. H. Jonsson (2012), Aerosol and gas re-distribution by shallow cumulus clouds: An investigation using airborne measurements, *J. Geophys. Res.*, *117*, D17202, doi:10.1029/2012JD018089.

Xiao, R., et al. (2009), Formation of submicron sulfate and organic aerosols in the outflow from the urban region of the Pearl River Delta in China, *Atmos. Environ.*, *43*(24), 3754–3763.

Yamaguchi, T., G. Katata, I. Noguchi, S. Sakai, Y. Watanabe, M. Uematsu, and H. Furutani (2015), Long-term observation of fog chemistry and estimation of fog water and nitrogen input via fog water deposition at a mountainous site in Hokkaido, Japan, *Atmos. Res.*, *151*, 82–92, doi:10.1016/j.atmosres.2014.01.023.

Youn, J. S., E. Crosbie, L. C. Maudlin, Z. Wang, and A. Sorooshian (2015), Dimethylamine as a major alkyl amine species in particles and cloud water: Observations in semi-arid and coastal regions, *Atmos. Environ.*, *122*, 250–258, doi:10.1016/j.atmosenv.2015.09.061.

Yuan, Q., W. J. Li, S. Z. Zhou, L. X. Yang, J. W. Chi, X. Sui, and W. X. Wang (2015), Integrated evaluation of aerosols during haze-fog episodes at one regional background site in North China Plain, *Atmos. Res.*, *156*, 102–110, doi:10.1016/j.atmosres.2015.01.002.

Zaveri, R. A., et al. (2010), Nighttime chemical evolution of aerosol and trace gases in a power plant plume: Implications for secondary organic nitrate and organosulfate aerosol formation, NO(3) radical chemistry, and N(2)O(5) heterogeneous hydrolysis, *J. Geophys. Res.*, *115*, D12304, doi:10.1029/2009JD013250.

Zelenyuk, A., D. Imre, M. Earle, R. Easter, A. Korolev, R. Leaitch, P. Liu, A. M. Macdonald, M. Ovchinnikov, and W. Strapp (2010), In situ characterization of cloud condensation nuclei, interstitial, and background particles using the Single Particle Mass Spectrometer, SPLAT II, *Anal. Chem.*, *82*(19), 7943–7951, doi:10.1021/Ac1013892.

Zhang, G. H., X. H. Bi, L. Y. Chan, L. Li, X. M. Wang, J. L. Feng, G. Y. Sheng, J. M. Fu, M. Li, and Z. Zhou (2012), Enhanced trimethylamine-containing particles during fog events detected by single particle aerosol mass spectrometry in urban Guangzhou, China, *Atmos. Environ.*, *55*, 121–126, doi:10.1016/j.atmosenv.2012.03.038.

Zhang, G. H., X. H. Bi, L. Li, L. Y. Chan, M. Li, X. M. Wang, G. Y. Sheng, J. M. Fu, and Z. Zhou (2013), Mixing state of individual submicron carbon-containing particles during spring and fall seasons in urban Guangzhou, China: A case study, *Atmos. Chem. Phys.*, *13*(9), 4723–4735, doi:10.5194/acp-13-4723-2013.

Zhang, G. H., X. H. Bi, J. J. He, D. H. Chen, L. Y. Chan, G. W. Xie, X. M. Wang, G. Y. Sheng, J. M. Fu, and Z. Zhou (2014), Variation of secondary coatings associated with elemental carbon by single particle analysis, *Atmos. Environ.*, *92*(0), 162–170, doi:10.1016/j.atmosenv.2014.04.018.

Zhang, R. Y., A. F. Khalizov, J. Pagels, D. Zhang, H. X. Xue, and P. H. McMurry (2008), Variability in morphology, hygroscopicity, and optical properties of soot aerosols during atmospheric processing, *Proc. Natl. Acad. Sci. U.S.A.*, *105*(30), 10,291–10,296, doi:10.1073/pnas.0804860105.